

Texturing, reflectivity, diffuse scattering and light trapping in silicon solar cells

Leonard Forbes

L. Forbes and Associate LLC, 7340 NW Mountain View Drive, PO Box 1716
Corvallis, OR 97339-1716 USA, lenforbes@forbes4.com, 1-541-753-1409

Abstract

The energy conversion efficiency is a critical consideration in the application of silicon solar cells. Texturing both front side and backside have been used to increase the absorption of infrared sun light energy in silicon solar cells. A review is given of some of the basic concepts and then a design described for the optimal textured structure and some of the practical limitations described in realizing this structure in silicon technology.

1.0 Introduction

Texturing and light trapping of infrared light energy are in reality old topics and the concepts and often discussed in relationship to silicon solar cells where the absorption coefficient of infrared light is very low. A separate but related issue has also been the use of texturing to reduce the reflectivity of silicon to visible light to improve particularly the blue response, this may not in general reduce the reflectivity to infrared light and if it does this will not result in infrared light trapping. The conflicting requirements for reduced reflectivity particularly for visible light and the requirement for light trapping of infrared light have often resulted in confusion among professionals working in the field of silicon solar energy. Light trapping requires high reflectivity of light at the internal side of the front surface for the light reflected from the backside of the solar cell.

A review is given of some of the basic concepts in terms of a simple model and then a design described for the optimal textured structure for infrared light trapping.

2.0 Front side and backside texturing

Texturing has been used as a technique to improve the efficiency of photodetectors and solar cells due to a reduction in reflections at the front surface. Most of the literature available describes the use of front side texturing of photodiodes to improve the absorption of visible light energy. Regularly textured front side surfaces have been described for solar cells by Arndt et al. (1975). The majority of silicon solar cells currently use single front side textured surfaces. Front side texturing not only serves to reduce the reflectivity of the silicon surface due to multiple attempts at transmission through the front surface as has been described by Arndt et al. (1975) but also results in longer path lengths for light that is scattered at large angles.

A light anti-reflecting region of pillars has also been described as an air-substrate index of refraction matching layer by Boden and Bagnall (2009) when considering the anti-reflecting characteristics of the “moth’s eye.” In some cases this anti-reflecting layer also acts like a light

diffusing layer with features configured to increase the effective absorption efficiency and energy conversion efficiency of the solar cell or photodetector. The anti-reflecting features may be cones, pyramids, pillars, and other features, and, when such features are used for diffusion and for the scattering of light may they be distributed in a random fashion. It should be noted that any feature that produces the desired diffusive light scattering is one that closely approximates a Lambertian scattering surface at the desired wavelengths of radiation. Lambertian scattering is ideal diffuse scattering providing light distributed over the whole half sphere or solid angle of 2π steradians. Manipulating the feature sizes, dimensions, etc. allows the light anti-reflecting and light diffusing region to be tunable for a specific wavelength. Varying the material near or deposited upon the anti-reflecting and light diffusing region can also be used to enhance these characteristics.

2.1 Front side texturing

Consider now the effect of front side texturing on the near infrared wavelength response where absorption is very low; texturing will also change the absorption in the remaining part of the infrared and the visible light regions but this will not yet be considered. In the near infrared the index of refraction of silicon is $n=3.42$ and the reflectance is about $R = 30\%$ from a single surface and transmittance through a single surface is $T = 70\%$ for normal incident waves. The absorption coefficient of silicon is very low in the near infrared. If there is no backside reflector radiation under normal incidence is reflected first from the first surface. There are successive reflections from both the back and internal reflections from the front surface resulting in a total transmittance, if there is no reflective layer or the oxide layer, of

$$T_{\text{tot}} = (T T) (1 + R^2 + R^4 + \dots) = (T T) / (1 - R^2) \quad (1)$$

This result has been obtained using the sum of a geometric series. If both top and back surfaces are just polished silicon-air then this results in a total transmittance of 54% and a reflectance of 46%. The internal absorption, A , of infrared light where the absorption coefficient, α , is very low due multiple internal reflections in a sample of thickness, d , with a polished backside is

$$A = \alpha d (1 + R_2)(1 + R_1 R_2 + R_1^2 R_2^2 + \dots) = \alpha d (1 + R_2) / (1 - R_1 R_2) \quad (2)$$

The enhancement, Enh , in internal absorption by multiple internal reflections with a polished backside is

$$Enh = (1 + R_2) / (1 - R_1 R_2) \quad (3)$$

The back surface can be coated with a thin oxide or conductive oxide and metal reflector to produce an internal reflection that is specular. If the backside is a perfect reflector, a condition that can't be achieved in general by placing metal directly on the semiconductor [3], but that can be achieved by metal over an oxide, then $R_1 = 0.3$ and $R_2 = 1.0$ and

$$Enh = (1 + R_2) / (1 - R_1 R_2) = 3 \quad (4)$$

and the external quantum efficiency, EQE is

$$EQE = \alpha d T_1 (1 + R_2) / (1 - R_1 R_2) = 2 \alpha d T_1 \quad (5)$$

where T_1 is the fraction of the incident light transmitted through the first surface, for specular reflections light $T_1 = (1 - R_1)$. However, for simplicity in further analysis and notation we will designate R_1 to be the fraction of light incident from the backside on the front surface and reflected back internally from the front surface. This need not be simply related as previously to the fraction of incident light transmitted from outside the sample through the front side surface.

Now consider the case as shown in Fig. 1(a) with a textured front surface and backside reflector. For simplicity if we neglect the increase in individual path lengths due to scattering by a textured front surface and count only the number of reflections then if the front side is textured and an antireflecting film added to minimize, $R_1 \sim 0$. If the reflectivity of the front surface to incident radiation is very low then the reflectivity to radiation incident from the backside is also very low. This results in only two passes of the incident radiation and then the $Enh = 2$ and $EQE = 2 \alpha d$. This underestimates the possible improvement possible due to front side texturing but apparently describes the where the front side is textured as porous silicon but there is little scattering (Yuan et al., 2009). Neglecting the increase in individual path lengths due to scattering by a textured front surface underestimates the improvement possible due to front side texturing but a more important practical consideration is the backside reflectivity. Estimates are that the reflectivity of aluminum directly on silicon may be as low as $R_2 = 0.3$.

If the absorption is not low then from Fig. 1(a) the absorption on two successive paths where, $R_1 \sim 0$, and, $R_2 = 1$, can be expressed as

$$A = (1 - \exp(-\alpha d)) (1 + \exp(-\alpha d)) = (1 - \exp(-2\alpha d)) \quad (6)$$

If the absorption, αd , is low, $A = 2 \alpha d$ and if the absorption is high, αd , is large, $A = 1$. Eqn. 6 will be used later in comparing the absorption due to front side texturing to the absorption due to backside texturing.

2.2 Backside texturing

Backside texturing, Fig. 1(b) has also been used as a technique to improve the efficiency of photodetectors and solar cells due to backside light scattering and light trapping by improving the absorption of near infrared light energy. Backside texturing can result in multiple internal reflections and light trapping. One of the first descriptions of using this technique in photodetectors was by St. John(1969). Another description was provided by Cotter (1998). A more recent description of the same technique on ultra-thin solar cells has been given by Aberle et al. (2007). They disclosed the use of white paint as the backside diffuse reflector. Their initial results show a large increase in the absorption with the white paint as a back

surface reflector but only a modest ten or twenty percent increase in the quantum efficiency. We have also investigated the use of white paint as a diffuse reflector (Forbes and Louie, 2010). A later result by Aberle et al. (2007) indicated that a twenty to forty percent enhancement in conversion efficiency can be obtained on thin film microcrystalline solar cells by adding more titanium dioxide to the white paint. However, thick layers of the order 80 μm or more of paint are required on thin film solar cells which in themselves are only a few micrometers thick.

If the increase in the individual path lengths caused by the diffuse scattering at the backside is neglected and if the absorption coefficient is very low then the total effective path length is determined by just the number of reflections. If then as before R_1 is designated to be the fraction of light incident from the backside on the front surface that is reflected back internally from the front surface, the total absorption can be shown to be

$$A = \alpha d (1 + R_2)(1 + R_1 R_2 + R_1^2 R_2^2 + \dots) = \alpha d (1 + R_2) / (1 - R_1 R_2) \quad (7)$$

The effective increase in absorption is $\text{Enh} = (1 + R_2) / (1 - R_1 R_2)$. The internal quantum efficiency, IQE, in the infrared where the absorption in silicon is low is then, $\text{IQE} = \alpha d \text{Enh}$. The external quantum efficiency, EQE, is $\text{EQE} = T_1 \text{IQE}$ and $\text{EQE} = T_1 \alpha d \text{Enh}$. T_1 is the fraction of light incident on the front surface from outside the sample that is transmitted through the front surface, 0.7, for an air-silicon interface.

A technique that improves the infrared response has the top side polished but the back side textured with an oxide like silicon oxide or transparent conductive oxides like zinc oxide, indium oxide, or tin oxide, and a metal like aluminum or silver or mirror reflector. The texturing is realized in a fashion to produce a true diffuse scattering, Lambertian scattering at infrared wavelengths. This diffuse scattering layer and reflecting layer combination, in essence, yields $R_2 = 100\%$, an ideal diffuse reflector. The reflectance of the polished front side to the scattered light radiation is determined by solid angle considerations. Any incident light with an angle of incidence greater than the critical angle θ , will be totally internal reflected. If the backside scattering is totally diffuse or Lambertian, the transmittance is then determined by the area of the surface, πr^2 , within the critical angle, θ , in this case 17° for silicon and air. The radius of the circle is $r = d \sin(17)$, where, d , is the thickness of the sample. This area is divided by the area of the half sphere, $2 \pi d^2$. If the backside scattering is totally diffuse the transmittance of the front planar surface is then roughly 3% to internally reflected light from the backside and the reflectance $R_1 = 97\%$. The path length enhancement factor can be very large

$$\text{Enh} = (1 + R_2) / (1 - R_1 R_2) = 66 \quad (8)$$

This would result in an internal quantum efficiency, $\text{IQE} = 66 \alpha d$ and since T_1 is still 0.7 and $\text{EQE} = 46 \alpha d$. This is consistent with the estimate by Cotter (1998) that was defined as, $4\eta^2$, where, η , is the optical index of refraction of the semiconductor, then for a backside textured silicon photodetector $4\eta^2 = 51$ in the near infrared where the index of refraction for silicon $\eta = 3.42$. If the backside is a textured and truly diffusive scattering surface and a mirror like

surface is used behind the back side, a very large enhancement of absorption in the near infrared can be achieved.

If the absorption in the silicon layer is not assumed to be small but rather taken into account it can be shown that the enhancement factor for the internal quantum efficiency due to multiple reflections is modified from Eqn. 8 and becomes

$$\text{Enh} = (1 - \exp(-\alpha d))(1 + R_2 \exp(-\alpha d)) / (1 - R_1 R_2 \exp(-2\alpha d)) \quad (9)$$

This allows a calculation of the responsivity, in terms of the electrical current in Amperes per incident light power in Watts, of solar cells of different thickness, d , for different wavelengths, λ , since the absorption coefficient, $\alpha(\lambda)$, is a function of wavelength. If it is assumed that the backside is an ideal reflector, $R_2 = 1.0$, and the amount of diffusive scattering of the back surface varies from that of a planar surface then the fraction of light reflected back from the front surface will vary. If the back surface is planar then there is only specular reflection and, $R_1 = 0.3$, if the back surface is an ideal Lambertian diffusive surface then the fraction of light reflected back from the front surface will be very large, $R_1 = 0.97$. Several values of R_1 are discussed herein for a diffuse reflector, these represent the fraction of light internally reflected back at the front surface. For purposes of the present description, values of $R_1 \geq 0.9$ are deemed particularly useful. The enhancement in absorption described by Eqn. 9 then varies with the fraction of light radiation reflected back from the front surface and thickness of the sample. These results are compared in Fig. 2(a) for a thin 2 micrometer thick sample to those for front side texturing as described by Eqn. 6. The same assumptions have been used in both cases with respect to radiation path length. As can be seen from the calculated responsivity in Fig. 2(a) backside texturing is much more effective in enhancing the absorption of infrared light energy.

The analysis for backside texturing can also be performed for thick silicon solar cells or photodetectors, and compared to published results by Yamamoto et al., (2010) in Fig. 2(b). Eqn. 9 has been used in this comparison where $R_1 = 0.93$, and $R_2 = 1.0$, indicating a very effective backside scattering by a laser ablated surface.

3.0 Practical realizations

3.1 Backside reflectors

One of the difficulties in silicon technology is realizing a backside reflector. Metal directly on a silicon backside has been found in practice not to be a good reflector. One approach in thin film technology has been to deposit silicon on an oxide over a textured metal. In doing so the desire has been to use thicker oxides to try to planarize the oxide top surface for silicon deposition. One of the difficulties with this approach is illustrated in Fig. 3(a), while the metal may be a diffusive reflector but the reflected light is defracted towards the normal upon entering the silicon. The light in the silicon will not appear to originate from a Lambertian scattering source. In Fig. 3(b) the backside of the silicon is textured and a thin oxide or dielectric is used before metal deposition. If the oxide is thin, much less than a quarter

wavelength then the reflected light is not affected by the thin oxide and the reflection into the silicon can be Lambertian scattering.

3.2 Diffuse light scattering

Diffuse scattering at even one wavelength is in general not easily achieved and is not realized by pyramidal structures, random pyramidal structures nor gratings. Ideal reflective Lambertian scattering provides light distributed over the whole half sphere or a solid angle of 2π steradians. Herein the use backside texturing provides diffusive reflective light scattering at the backside and planar front side surfaces to provide for total internal reflections at the front side and multiple passes of red and infrared light in silicon solar cells. The front surface preferably has an anti-reflecting layer for visible light, but this layer does not significantly effect the reflectivity of the front surface to infrared light.

Thus, a solar cell or photodetector has been described that provides optimal conversion of visible light and infrared energy to electricity. Backside texturing with diffusive scattering and frontside internal reflection produce a large enhancement of conversion efficiency. The preferred structure uses a set of cusps etched into the backside of solar cells to provide diffusive scattering. One of the best examples of the scattering and diffraction of light is the classical treatment of the interaction of light with narrow slits such as given by Born and Wolf (1999). Here we will replace the slits by reflective strips in an absorbing material. Consider firstly light of one particular wavelength, or wavenumber, k . For an array of n strips of width, s , and equal spacing, d , with the light vertically incident, the intensity of the diffracted light on a screen, I , is proportional to:

$$I \sim (H(n d k p / 2) \text{ sinc}(s k p / 2))^2 \quad (10)$$

where $\text{sinc}(x)$ is the ratio, $\sin(x)/x$, and $p = \sin \theta$, θ is the angle from the vertical at which the light is diffracted. The formula for the intensity is valid if the observing screen is much farther away than, s or d , or namely the Fraunhofer diffraction regime. In this case, the diffraction pattern is equivalent to the Fourier transform of the diffraction grating. For a single strip of finite width, the diffraction pattern has the well-known form of a sinc function. For multiple slits of finite width, the diffraction is a pattern of peaks and troughs of the aperture, $n d$, whose locations are described by the interference function, H , and whose intensity is modulated by the sinc function pattern arising from a single strip. The envelope of the intensities of the regular diffraction pattern observed on the screen is a sinc function. An alternative derivation to that in Born and Wolf (1999) given by Falloon (2011) is to firstly recognize that a set of narrow strips are described by the convolution of a series of delta functions with a single strip so the Fourier transform of the grating is the product of the transform of a series of delta functions, which yields H , times the Fourier transform of a single strip the sinc function, $\text{sinc}(s q / 2)$. This yields $H \sim \sin(n d q / 2) / \sin(d q / 2)$. Here, q , is the normalized wave number, $q = k p = k \sin \theta$.

Consider now a solar cell as shown in Fig. 4, where light incident on the top or front surface passes through the cell and strikes a textured reflective surface at the bottom or back of the cell, Fig. 4(b). Lambertian scattering by a single element into a semicircle will, as shown in Fig. 4(b), result in a Lorentzian intensity pattern, Fig. 4(a) on a flat screen. Light will be scattered large distances in the, x , direction as a result of the uniform intensity on the semicircle. Here the normalized wavenumber is, $q = k_p = k \sin(\theta)$. In order to achieve Lambertian scattering then one must find the inverse Fourier transform of the Lorentzian and use this for the shape of a single element providing scattering or for each element providing diffraction in an array. The Fourier transform of each element providing scattering will then give uniform illumination of a semicircle and a Lorentzian shape on the flat screen. The inverse Fourier transform of a Lorentzian is a "cusp" as shown in Fig. 4(c). A series or array of strips of such regular "cusps" will result in a series of dots on the screen with a nearly uniform intensity described by a Lorentzian envelope for the intensities over a wide range of distances, each dot will have the shape and location described by the interference function, H , of the aperture defining the region occupied by the "cusps." A regular array of strips of cusps will produce a regular diffraction pattern of dots on the front surface where the intensity is determined by the Fourier transform of the single "cusp" shown in Fig. 4(a). It is fairly straightforward to demonstrate this in two dimensions in a qualitative manner by considering an array of strips of cusps and using numerical calculations on a computer that does Fourier transforms. This has also been illustrated in Fig. 5(a) as was experimentally shown by Born and Wolf (1999) by illuminating a aperture with punched holes, top illustration, on a dark screen as in the bottom part of each illustration. Likewise an random array of "cusps" will also work as well, these will produce a random array of dots on the front surface or a "fuzzy" pattern as shown in Fig. 5(b) as was experimentally shown by Born and Wolf (1999).

In the case of a solar cell with very wide features there is essentially no aperture. A regular array or random arrangement of strips of "cusps" on the backside will result in Lambertian scattering from each element separately and optimal scattering. In the case of solar cells there need be no concern about the accumulative effect of a large number of "cusps" and whether or not they form a regular diffraction pattern. We need only be concerned here that the scattering from each element be Lambertian, this will insure a maximum of total internal reflection back from the silicon side of the front surface. The solar cells are however three dimensional, to affect a practical realization of the "cusp" features we need to rotate the cusps to give scattering in three dimensions. It is easier to make random isolated individual "cusps" rather than strips of "cusps".

The size of the "cusps" are chosen to optimize a particular wavelength, λ , the wavelength in silicon. For instance, $1/a$, the height of the "cusps" is chosen to be some multiple factor of the wavelength. The maximum slope for a normalized cusp is minus one so the maximum scattering angle is ninety degrees. Since the height of the cusps does not have to be any particular multiple factor of the wavelength for nearby infrared wavelengths the scattering will also be Lambertian. For infrared sunlight energy the scattering from each cusp in a random

array will be diffusive or nearly diffusive scattering resulting in light trapping (Forbes 2011) and a significant increase in the conversion efficiency of solar silicon cells.

4.0 Conclusions

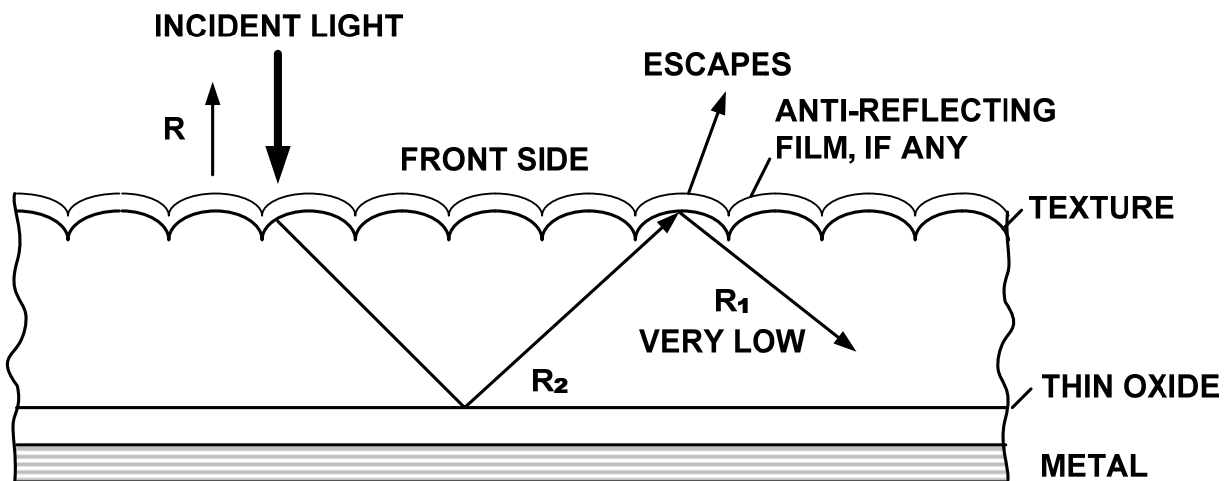
A random array of such etched “cusps” into the backside of a silicon wafer can be provided by porous silicon and chemical etches. A porous silicon or metal catalyst etch can provide vertical holes at random locations, these can then be etched with a conventional isotropic silicon etch to round off the shape corners resulting in a cusp like structure. A thin layer of oxide can either be grown or oxide or another dielectric deposited and the backside covered by a reflective metal. In this manner a random array of cusp like scattering centers can be formed on the back of silicon solar cells.

Backside texturing and reflective structures have the potential of making large improvements in the energy conversion, from 10% to 20% on thick crystalline or multi-crystalline silicon (Forbes and Louie 2010) and from 20% to 40% on thin film microcrystalline and amorphous silicon (Aberle et al., 2007) solar cells. Backside texturing and light trapping may be necessary to realize the full potential of thin film silicon solar cells in comparison to other competitive technologies as is evident from the review by Razykov et al. (2011).

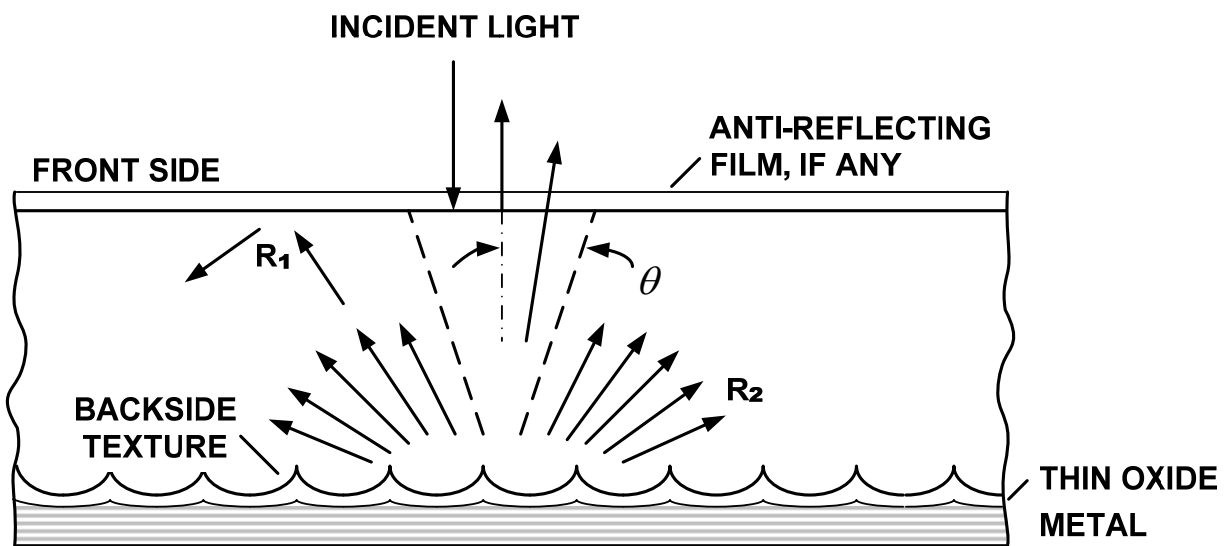
References

- Aberle, A. G., Berger, O., and Inns, D., 2007. Commercial white paint as back surface reflector for thin-film solar cells. *Solar Energy Materials & Solar Cells*. 91, 1215–1221.
- Arndt, R.A., Allison J.F., Haynos, J.G., and Meulenber, Jr., A., 1975. Optical properties of the COMSAT non-reflective cell. 11th IEEE Photovoltaic Spec. Conf. 40-43.
- Boden, S.A., and Bagnall, D.M., 2009. SPIE Optics and Photonics. Nanostructured biomimetic moth-eye arrays in silicon by nanoimprint lithography. *SPIE Optics and Photonics*. 74010J-1 - 74010J-12.
- Born, M., and Wolf, E., 1999. *Principles of Optics*, seventh ed. Cambridge University Press, Cambridge, pp. 446-455.
- Cotter, J.E., 1998. Optical intensity of light in layers of silicon with rear diffuse reflectors. *J. Appl. Phys.* 84, 618-624.
- Forbes, L., and Louie, M.Y., 2010. Backside Nanoscale Texturing to Improve IR Response of Silicon Photodetectors and Solar Cells. *Nanotech.* 2, 9-12.

- St. John, A.E., 1969., Multiple Internal Reflection Structure in a Silicon Detector which is Obtained by Sandblasting. U.S. Patent 3,487,223.
- Razykov, T.M., Ferekides, C.S., Morel D., Stefanakos E., Ullal, H.S., and Upadhyaya, H.M., 2011. Solar photovoltaic electricity: Current status and future prospects. Solar Energy. 85, 1580-1608.
- Yamamoto, K., Sakamoto, A., Nagano, T., Fukumitsu, K., 2010. NIR sensitivity enhancement by laser treatment for Si detectors. Nuclear Instr. and Meth. Phys. A624, 520-523.
- Yuan, H.-C., Yost, V.E., Page, M.R., Stradins, P., Meier, D.L., and Branz, H.M., 2009. Efficient black silicon solar cell with a density-graded nanoporous surface: Optical properties, performance limitations, and design rules. Appl. Phys. Lett. 95, 123501.
- Falloon, P., "Multiple Slit Diffraction Pattern" from the Wolfram Demonstrations Project <http://demonstrations.wolfram.com/MultipleSlitDiffractionPattern/> last accessed July 2011.
- Forbes, L., 2011. Continuation in Part of US Patent Publication 201110140106 Backside texturing by cusps to improve IR response of silicon solar cells, to be published Dec. 2012. <http://appft1.uspto.gov/netathtml/PTO/search-adv.html> last accessed July 2011.

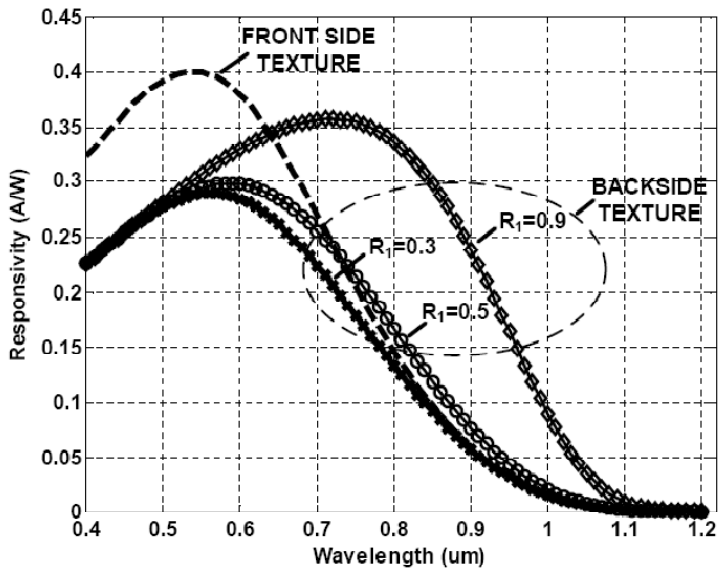


(a)

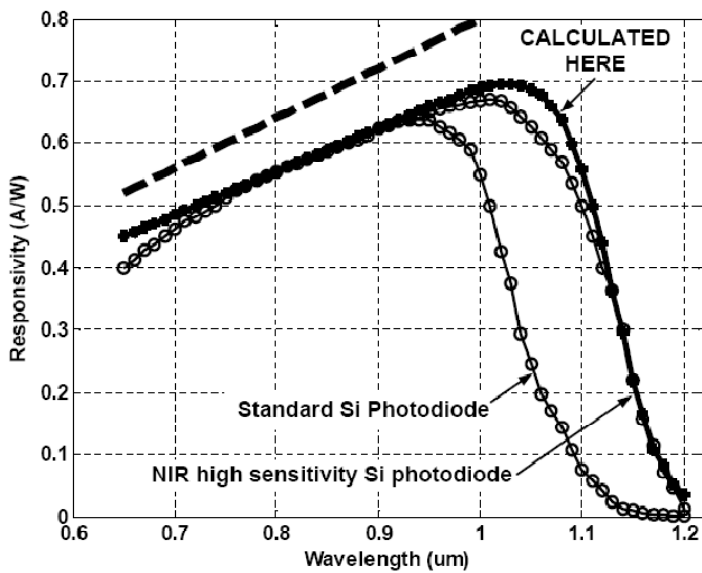


(b)

Fig. 1. (a) Front side textured solar cell,
(b) Backside textured solar cell.

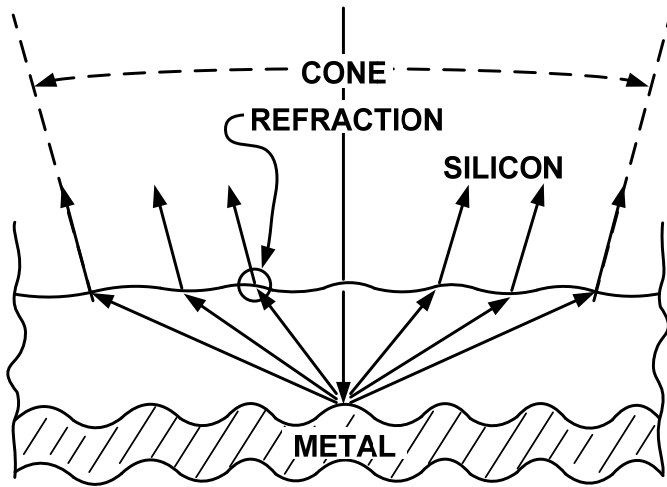


(a)

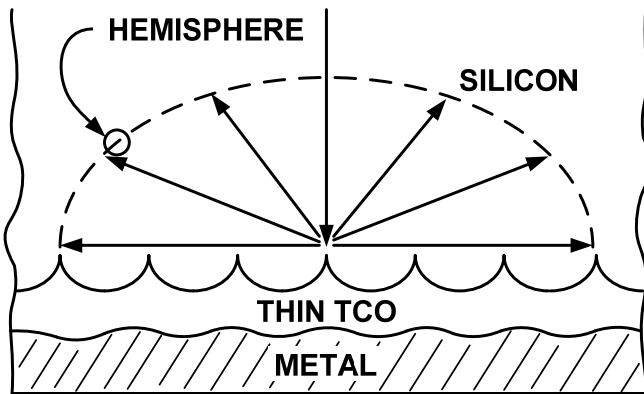


(b)

Fig. 2 (a) Comparison of front and backside texture on thin film silicon solar cells , (b) Matching of our model with $R_2=1$ and $R_1=0.93$ to data by Yamamoto et al.,(2010) 270 μm silicon wafer, backside texture.

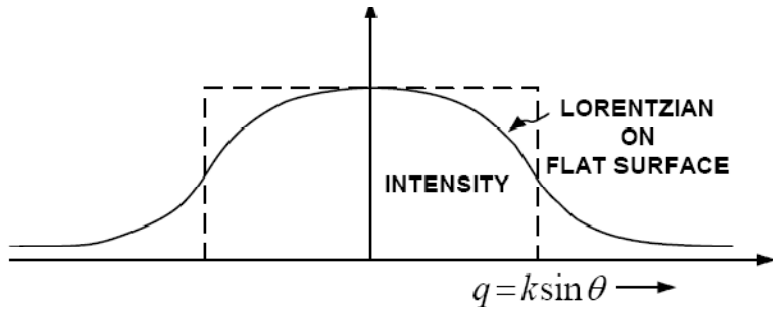


(a)

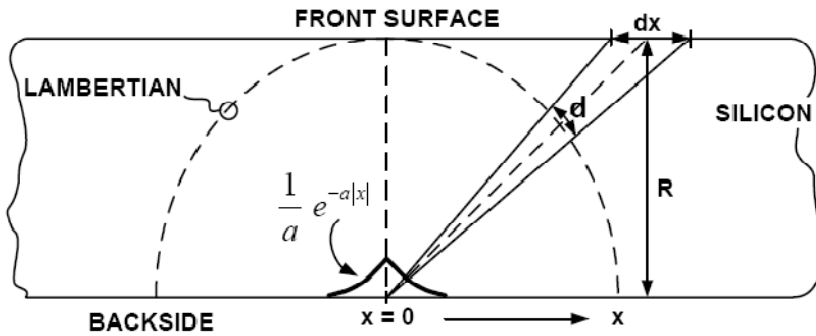


(b)

Fig. 3. (a) Silicon grown on textured metal,
 (b) Metal reflector deposited on the backside of textured silicon.



(a)

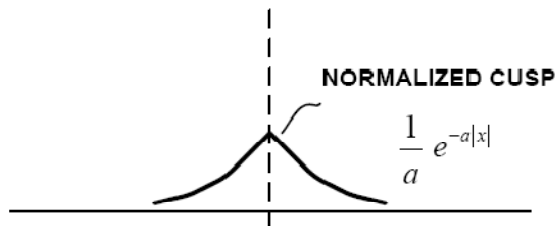


(b)

AREAS

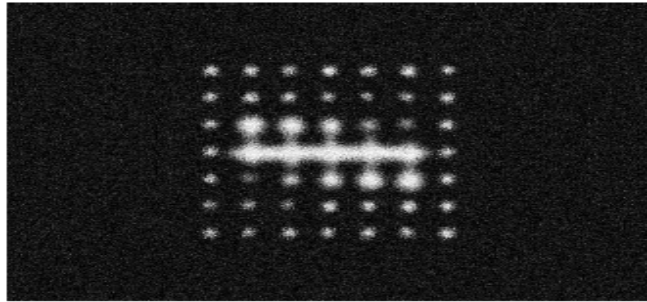
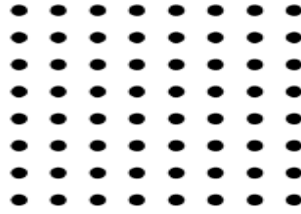
$$\frac{d dz}{dx dz} = \frac{1}{1 + \left(\frac{x}{R}\right)^2}$$

$$FT \left(\frac{a}{2} \cdot e^{-a|x|} \right) = \frac{1}{1 + \left(\frac{k}{a}\right)^2}$$

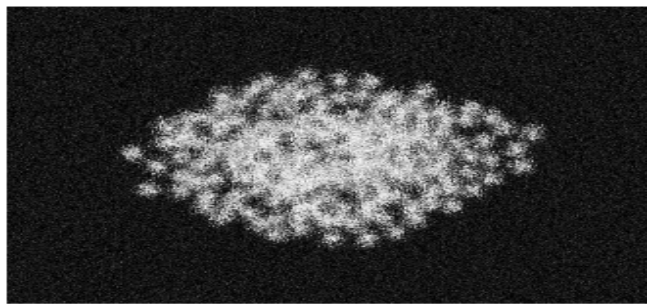
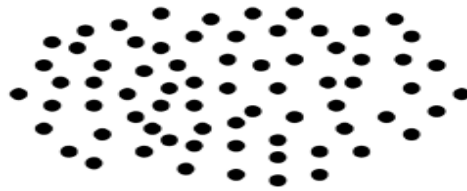


(c)

Fig. 4. (a) Scattered light amplitude at front side,
 (b) Light scattering by backside texture,
 (c) Normalized cusp and Fourier transform.



(a)



(b)

Fig. 5. (a) Diffraction pattern of a regular array,
(b) Diffraction pattern of a random array.